

Ciliary Propulsion

In the previous section we discussed the hydromechanics of locomotion in organisms propelled by individual flagella or flagellar bundles. In some organisms with more than one flagellum the hydromechanical analysis could proceed along similar lines provided the hydrodynamic interactions between the flagella are relatively weak. However, there are organisms with more than one flagellum that seemingly derive a beneficial propulsive effect by adjustment of the phase relationships of the beat patterns of their “flagella”, for example *Mixotricha* (Cleveland & Cleveland 1966) and *Volvox* (Hand & Haupt 1971). It appears that such beneficial interactions can also accrue to groups of individual organisms swimming close to one another; there are clearly analogous natural phenomena at high Reynolds numbers in the flight patterns of groups of birds and in the schooling of fish (Weihs 1975).

Cilia are essentially short flagella that (1) may beat back (recovery stroke) and forth (effective stroke) at different rates transcribing what is known as a “polarized” beat or (2) that may oscillate in a manner indistinguishable from “eukaryotic flagella.” They occur in large arrays, such as “ciliated epithelium” and produce fluid motion by collaborative action arising from a definite phase relationship between the beats of neighboring cilia. The presence of such a relationship is known as metachrony and often results in a wave, known as a metachronal wave, traveling over the array. It may be that ciliary systems evolved from flagella because of the beneficial hydrodynamic effects of the interactions of the cilia.

Cilia occur throughout the animal kingdom and indeed are extensively used not only for producing fluid motion but also for sensing motion. Examples of the former use are the cilia in the gills of non-motile marine animals used for ingestion of water (Mello & Sleigh 1972, Sleigh & Aiello 1972), and the cilia lining the trachea and lungs that provide a cleaning mechanism by continuously propelling mucus up and out of the lungs. Figure 1 is an electron micrograph of the cilia of frog lung mucosa. Cilia also line the oviduct

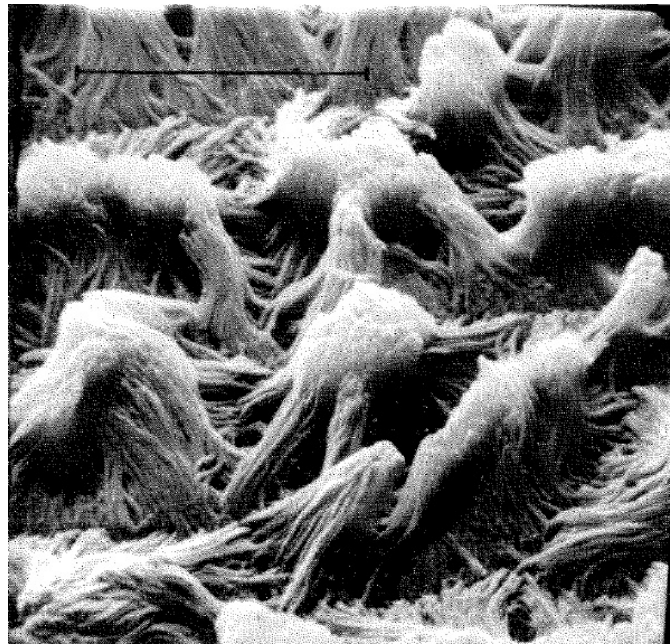


Figure 1: A scanning electron micrograph of frog respiratory mucosa. These fixed organelles display a typical metachronal pattern that reflects the beat-rhythm orientation. Scale bar is $10\mu m$. Photograph by P.P.C.Graziadei.

and contribute to the transport of the ova in that organ (Halbert, Tam & Blandau 1976; see also Dirksen &

Satir 1972); the uterine wall is ciliated and the fact that spermatozoa appear to swim close to this wall may be because they derive a beneficial effect from the beating cilia. In addition, the cilia on the membrane lining the ventricles of the brain (the ependyma) have been shown to create sufficient local mixing to affect the thickness of the so-called unstirred layer, thereby enhancing the diffusion or transport of ions across the membrane (Nelson 1975).

There are other functions in which motile cilia play a major role. So-called sensory cilia tend to be non-motile and often display a “9 + 0” microtubular axoneme. They are found in sensory organs devoted to photoreception or “eyes”. The flagellum of some protozoa may also be part of (1) a photoreceptor system (see Hand & Haupt 1971) (2) a chemoreceptor system or olfactory organs (see Reese 1965), or (3) a mechanoreceptor system adapted for detection of sound, touch, or orientation in a gravity field. The importance of ciliary systems even extends into ecological areas. For example, an individual California mussel *Mytilus californianus* can remove a significant amount of suspended mud and other matter from water, given an average filtration rate of 2.6 l of water per hour through its cilia-lined gills (Fox & Coe 1943).

But perhaps the ciliary systems most readily observed are those that provide propulsion for eukaryotic cells (e.g. Figures 2 and 3). From a hydrodynamic point of view these systems are more readily understood

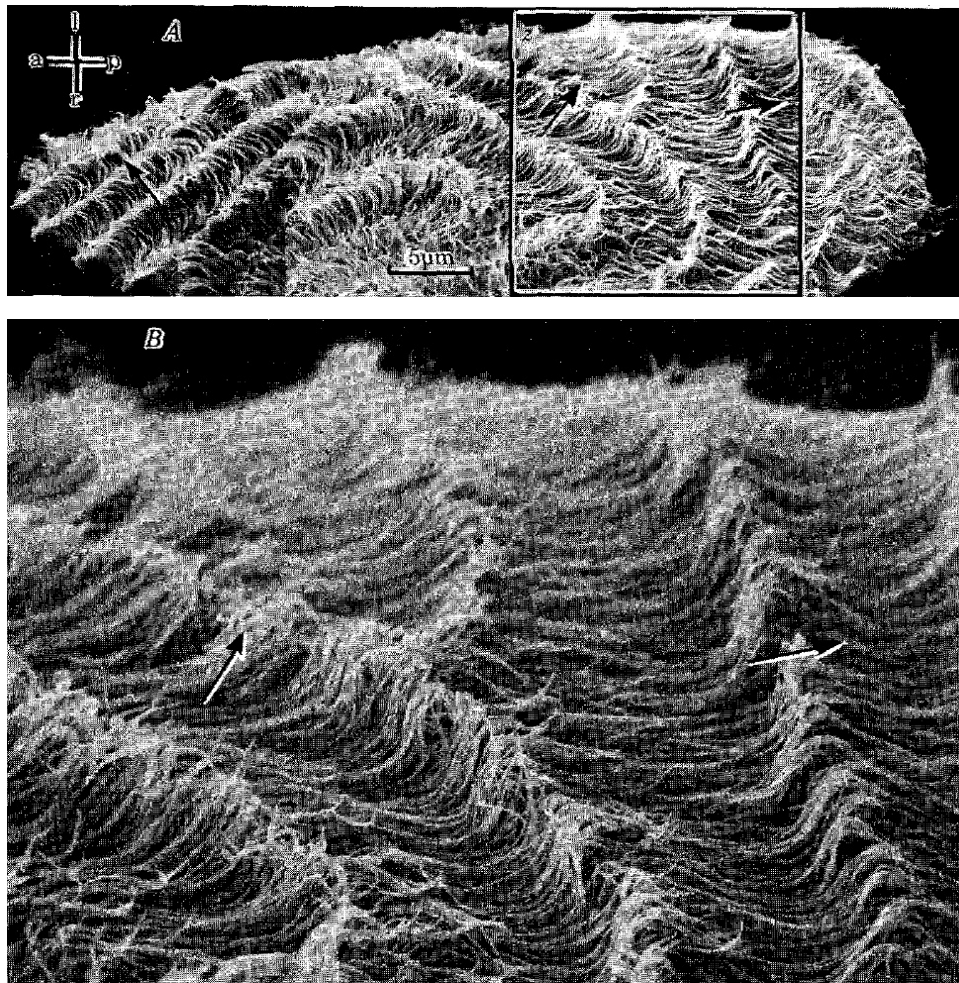


Figure 2: A scanning electron micrograph following rapid fixation of the ciliated protozoan *Opalina*. The in vivo metachronal wave orientation is reflected in the pattern over the fixed specimen. Arrows indicate the directions of the metachronal wave. Photograph by Tamm & Horridge (1970).

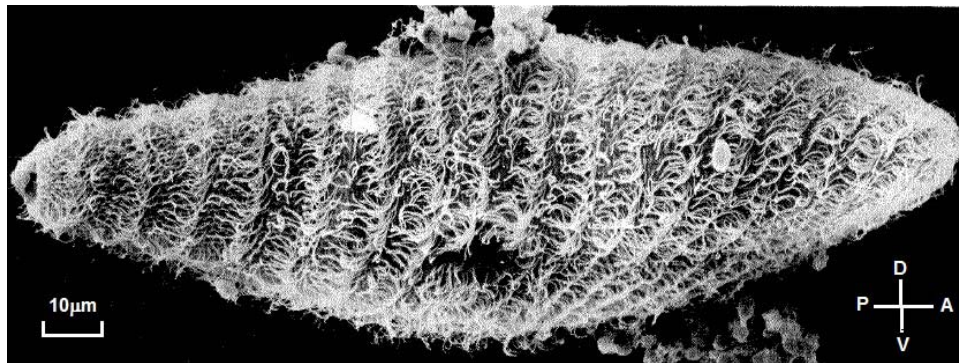


Figure 3: A scanning electron micrograph following rapid fixation of the ciliated protozoan *Paramecium*. The metachrony of this specimen is dexiopectic and/or antiopectic. In the inset A-P is the anterior-posterior axis and D-V the dorsal-ventral sides. Photograph by Tamm (1972).

because the fluid is usually Newtonian. On the other hand, the fluid in mammalian ciliary systems is often highly non-Newtonian (e.g. the mucus in the lung).

Each individual cilium usually has a fairly regular beat pattern (see, for example, Sleight 1960, 1962, 1968, 1972, 1973, 1974c; Parducz 1967) that often appears to be created by the propagation of a bend from the base to the tip of the cilia as illustrated by the beat pattern for *Opalina* in Figure 4. That phase of

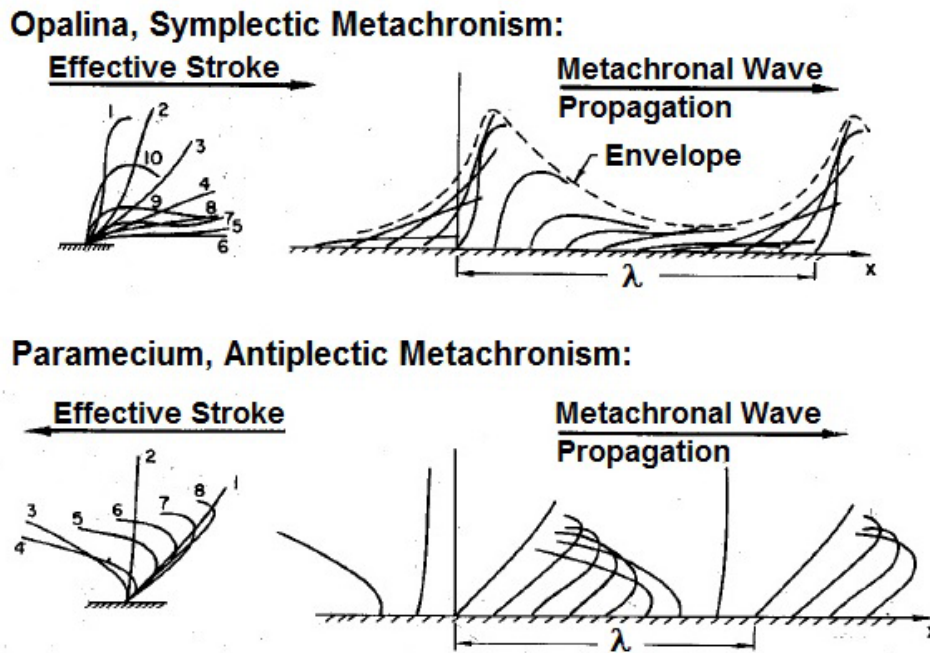


Figure 4: Approximate beat patterns for *Opalina* and *Paramecium* with the positions of an individual cilium at equal intervals in time on the left and the positions of an array of cilia at a given time on the right, showing the symplectic metachronism of *Opalina* and an antiopectic approximation to the metachronism of *Paramecium*. From Brennen and Winet (1977).

the beat in which each cilium is moving in a general direction so as to propel the organism is termed the effective stroke. Generally the cilium is straightened out during this phase and in the remainder of the beat known as the recovery stroke the cilium sneaks back to its starting point in a bent position so that a significant portion of each cilium is moving tangential to the fluid rather than normal to it as in the effective stroke. Such asymmetry immediately suggests that the cilia are taking advantage of the difference in the force coefficients for flow normal and tangential to a slender body. Furthermore, the motion is often

three-dimensional with some recovery motion taking place out of the plane of the effective stroke, as is the case with *Paramecium* (Machemer 1972a,b; Tamm 1972). While precise information on the ciliary beat pattern represents necessary data prior to any hydrodynamic analysis, it is difficult to obtain from light microscopy studies.

Often eukaryotic cilia ensembles exhibit metachrony: in one surface direction a cilium beats slightly out of phase with its neighbor so as to produce a metachronal wave (velocity, c) traveling over the surface (see Figure 2). To add to the complexity the direction of wave propagation may have almost any orientation relative to the direction of the effective stroke. Knight-Jones (1954) coined a series of terms to identify this relationship: when the metachronal wave propagation and the effective stroke are in the same direction, this is known as symplectic metachronism; if they are in opposite directions, it is termed antiplectic; and if the directions are normal to one another they are termed diaplectic (dexioplectic if the rotation from the metachronal wave direction to the effective stroke direction is 90° anticlockwise viewed from above and laeoplectic if 90° clockwise. Symplectic metachronism is illustrated by the electron micrograph of Figure 2 (Tamm & Horridge 1970) and the upper part of Figure 4 for *Opalina*; the lower part of Figure 4 represents an antiplectic approximation to the beat pattern of *Paramecium*, which does, however, contain a dexioplectic component as indicated in the electron micrograph of Figure 3 (Tamm 1972). On the other hand, there are ciliary systems in which metachrony is indiscernible. For example, Cheung & Jahn (1975) could not detect any organized metachrony in rabbit tracheal cilia; conversely a scanning electron micrograph from Graziadei (1971) of the cilia in the lung mucosa of the frog shows clear metachronism (Figure 1).

Many organisms have an avoidance response in which they reverse the direction of metachronal wave propagation and thus their direction of motion, a phenomenon known as ciliary reversal (Jahn 1975). This appears to be linked to their longitudinal electropotential gradient since it can be achieved by external imposition of an electrical potential. Other organisms such as *Opalina* appear able to vary continuously the direction of wave propagation and thus achieve greater maneuverability (Sleigh 1962). These responses in organisms with no identifiable and separate nervous system merely serve to highlight one of the great puzzles of ciliary systems, namely how these delicate phase relationships between the cilia are controlled. If one had to build a mechanical model to simulate such a system it would be extremely difficult, which probably accounts for the singular lack of mechanical model studies (the early work of Miller (1966) is the only work of this kind that we are aware of). Nervous control of ciliated epithelium is one of the important problems to which these studies may be applied.

In the following sections we confine ourselves to the hydromechanics of ciliary systems. We would, however, be remiss in not mentioning the important work in which attempts have been made to recover the internal motive force for ciliary beat patterns by working backwards from the known motion, the hydrodynamic forces and the presumed elastic structure of the cilia (Holwill 1966a, Harris 1961, Sleigh & Holwill 1969, Rikmenspoel & Sleigh 1970, and Rikmenspoel 1975).

The fluid mechanics of ciliary systems is clearly quite complex and most of the detailed and quantitative analyses have been based on simplifying assumptions concerning the interaction of the cilia and the fluid. Most of these studies have concentrated on what we shall term local fluid/cilia interaction models; for these purposes most authors have considered an infinite flat surface upon which the cilia motions are spatially and temporally periodic so as to form metachronal waves. The manner in which such solutions should be applied to finite, ciliated organisms is not entirely obvious; we return to this later. For the present, we discuss the two principal kinds of local fluid/cilia interaction models, the so-called envelope and sublayer models.

The Envelope Model

The envelope model assumes that the cilia are sufficiently closely packed together, as in the case of *Opalina* in Figure 2, so that the fluid effectively experiences an oscillating material surface. This envelope is commonly assumed to be impenetrable and the motion of each “particle” on the surface is assumed to be roughly equivalent to the locus of the tip of an individual cilium. An analysis of the low- Reynolds-number flow due to such an oscillating sheet was made by Taylor (1951) as a rough two-dimensional model for flagellar propulsion; thus Taylor only pursued the solution in which the “particles” had motions normal to the plane of the surface. Subsequently, in a short note, Tuck (1968) delineated the nature of the solution in which the oscillatory motions were purely tangential to the surface. Since then, solutions of a more general kind with oscillatory particle motions or ciliary loci of more general form have been produced by Reynolds (1965), Blake (1971b), and Brennen (1974). Consider an arbitrary elliptical form for the ciliary tip locus (Figure 5) in which the tip performs a simple harmonic motion of amplitude h_s tangential to the surface and

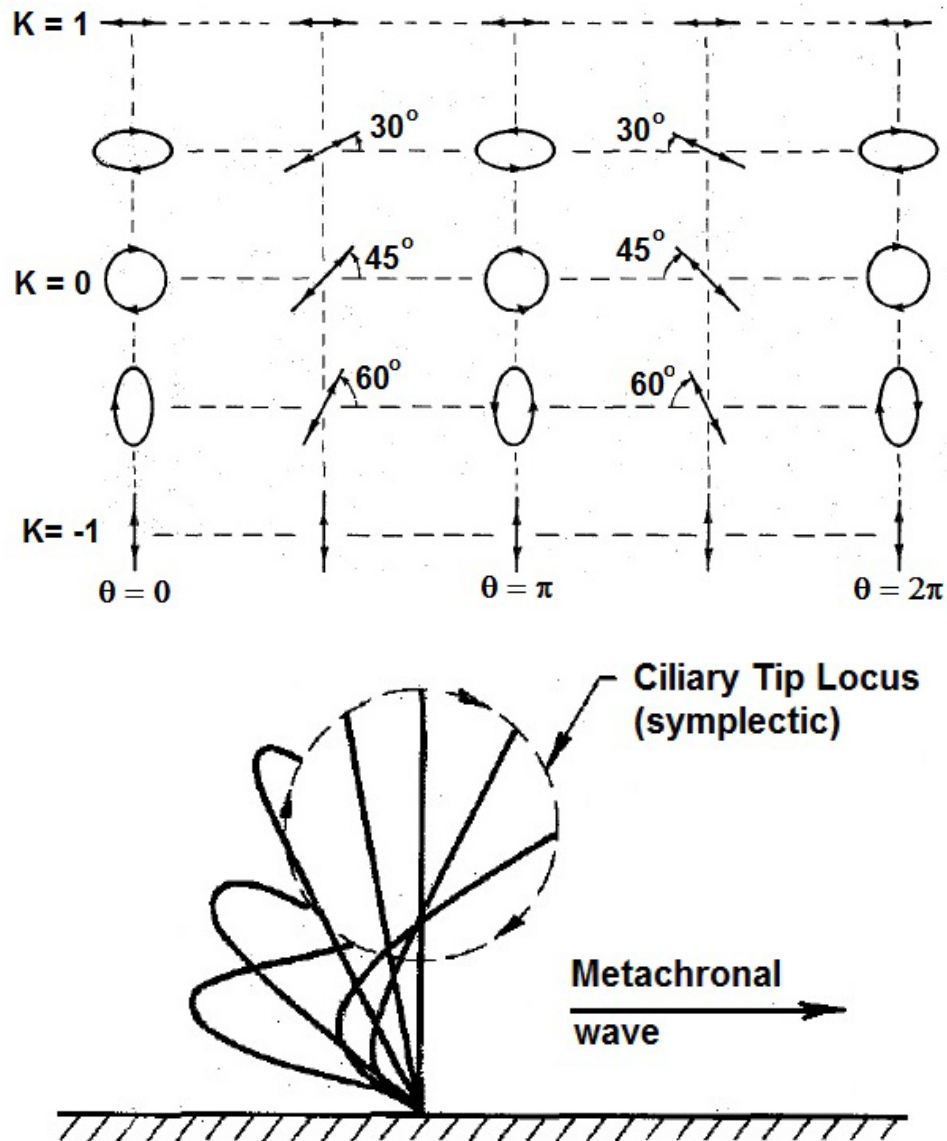


Figure 5: Variations of arbitrary elliptical ciliary tip loci with the parameters K and θ . The figure is correlated with the cell surface horizontal, the fluid above it and the metachronal waves traveling to the right. An example of a ciliary tip locus (symplectic) is indicated in the lower part of the figure. From Brennen and Winet (1977).

a simple harmonic motion of amplitude h_n normal to the surface. These deflections of frequency ω have a linear phase shift in the s direction along the surface so as to produce a metachronal wave of velocity, c , and

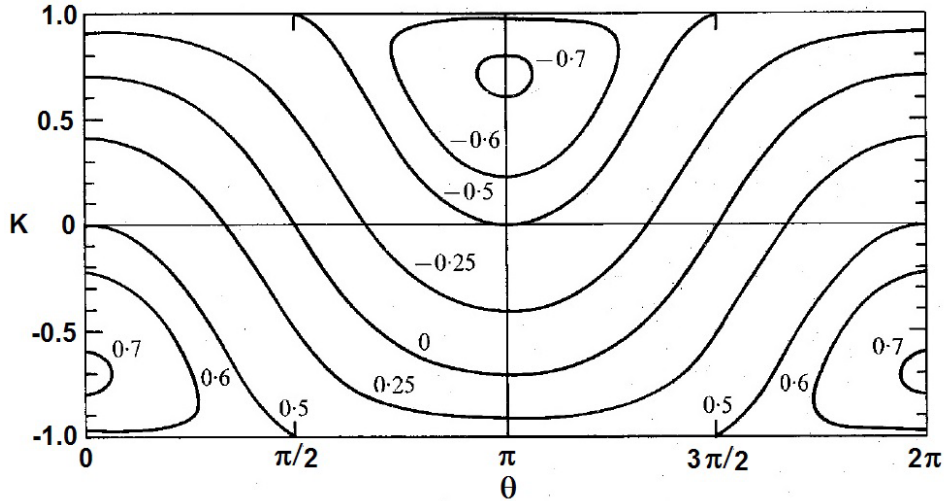


Figure 6: Variation of the dimensionless propulsive velocity $U/ck^2(h_s^2 + h_n^2)$ with the ciliary tip locus parameters K and θ according to the envelope model result (Dfh3); Contours are shown for various labeled values of $U/ck^2(h_s^2 + h_n^2)$; the figure should be used in conjunction with Figure 5.

wavelength, $\lambda(k = 2\pi/\lambda)$, traveling in the positive s direction. The mean position of the material surface (and thus of the cilium) is fixed in this frame of reference. Far from the envelope these oscillatory motions produce a rectilinear translation of the fluid tangential to the sheet whose magnitude in the positive s direction we shall denote by U . At any point, s , the motion tangential to the surface leads the motion normal to the surface by a phase angle $(\theta - \pi/2)$ and we define a parameter $K = (h_s^2 - h_n^2)/(h_s^2 + h_n^2)$. Then the various cilia loci that are so described are indicated diagrammatically in Figure 5. Note that $K = -1$ corresponds to Taylor's (1951) solution, whereas $K = +1$ corresponds to Tuck's (1968) solution. Brennen (1974) has shown that, provided the amplitudes h_s and h_n are small compared with the wavelength λ and the Reynolds number $Re = \omega/k^2\nu$ is small, the translation velocity, U , is given by

$$\frac{U}{c} = \frac{k^2}{2}(h_s^2 + h_n^2) \left\{ \frac{(\beta + 1)}{2\beta}(1 - K^2)^{1/2} \cos \theta - \frac{(\beta - 1)}{2\beta} - K \right\} \quad (\text{Dfh1})$$

where

$$\beta = \left\{ \frac{1}{2} [(1 + Re^2)^{1/2} + 1] \right\}^{1/2} \quad (\text{Dfh2})$$

Notice that this steady translation is quadratic in the dimensionless amplitudes kh_s and kh_n ; since these are assumed small, the velocity U is much smaller than the oscillatory velocities produced by motion of the envelope, which are first-order in kh_s and kh_n and which, incidentally, decay like e^{-kn} with normal distance, n , away from the envelope. The translation, U , arises from two different quadratic combinations of first-order oscillatory terms. The first and most important is in the quadratic term of the Taylor series expansion through which the velocity conditions on the envelope are satisfied. The second quadratic term is $O(Re)$ smaller and arises from the inertia terms in the Navier-Stokes equations. The latter disappears, therefore, when $Re \rightarrow 0$ and then

$$\frac{U}{c} \rightarrow \frac{k^2}{2}(h_s^2 + h_n^2) \{ (1 - K^2)^{1/2} \cos \theta - K \} \quad (\text{Dfh3})$$

which is in agreement with Blake's (1971b) results. The variation of the propulsion velocity, U , with the (K, θ) parameters was investigated by Brennen and is shown in Figure 6 in which contours of constant $U/ck^2(h_s^2 + h_n^2)$ are plotted. Notice that this exhibits two optimum forms for the ciliary locus. When $K = -2^{-1/2}$ and $\theta = 0$ a maximum propulsive velocity of $2^{-1/2}ck(h_s^2 + h_n^2)$ is achieved in the, positive s direction,

a situation that corresponds to symplectic metachronal propulsion. A simple Galilean transformation to bring the fluid at infinity to rest models a ciliate traveling in a direction opposite to the direction of wave propagation. On the other hand, maximum antiplectic propulsion of the same magnitude can equally well be achieved with a ciliary tip locus for which $K = 2^{-1/2}$, $\theta = \pi$ (see Figure 5). The energy expenditure per unit surface area, \dot{E} , for these motions is simply given by $\mu c^2 k^3 (h_s^2 + h_n^2)$. It follows that the above optima are also the most efficient means of propulsion in terms of propulsive velocity per unit energy expenditure per unit area. Finally, we note that calculations based on the expression (Dfh1) for non-zero Reynolds number indicate that even when Re is of order unity, the contours are little changed from those of Figure 6 (Brennen 1974).

Envelope models of this kind have been applied to a wide variety of physiological situations. Blake (1971b) and Brennen (1974, 1975) considered their application to the locomotion of ciliated microorganisms. Katz (1972) and Shack & Lardner (1972) used the method to model the propulsion of fluid in the ciliated tubes of mammalian reproductive systems, both female and male (see also Blake 1973b). In this regard considerable attention has been given to the role of the cilia in the mammalian oviduct in propelling the ovum. Ross (1971) has also used an envelope model to study the propulsion of mucus by the ciliated epithelium of the trachea. Such analyses have much in common with peristaltic pumping (Jaffrin & Shapiro 1971) where the “envelope” is a real material surface; in this case, considerations of and conditions upon the extensibility of the envelope are often imposed.

Apart from other more general problems to be discussed below, one of the major difficulties in comparing results from envelope model analyses with observations is that most of these analyses are limited to amplitudes h_s and h_n that are small compared with the metachronal wavelength, λ ; that is, kh_s and kh_n are small. On the other hand most ciliary systems appear to operate with values of kh_s and kh_n that are of order one or greater. This point is exemplified by the data presented in Figure 7, where values of U/c are compared with $k\ell$, ℓ being the cilia length; for purposes of comparison with the expression (Dfh3) and Figure 7 we may note that for many real ciliary beat patterns $\ell^2 \approx 4(h_s^2 + h_n^2)$. Blake (1971b) investigated envelope analyses for larger amplitudes by evaluating higher-order terms in kh_s , kh_n . But further nonlinear analyses that also incorporate higher-order harmonics in time in order to model the differences in the speeds of the “effective” and “recovery” strokes, are probably necessary before a conclusive evaluation of the utility of envelope models can be made.

Sublayer Models

A second distinct set of models has been proposed and developed for ciliary systems. These models concentrate on the interactions between individual cilia with the surrounding fluid and hence deal specifically with the flow among the cilia. For this reason they have been termed sublayer models. Blake (1972) first proposed such an analysis for the flow created by a regular array of cilia beating metachronously on an infinite plane wall.

By considering the relative motion between an element of a cilium and the surrounding fluid, sublayer models seek to establish the incremental force (or stokeslet strength) on each and every cilium element through use of resistive-force theory (section (Ble)). The entire flow field, denoted by its velocity $\underline{q}(\underline{x})$ where \underline{x} is a position vector, is then considered as having been created by this distribution of stokeslets and can be formally represented as an integral of the velocities induced at each point by each cilium element. Since these slender bodies operate close to a wall, the effect of the image system of singularities must also be included in order to satisfy a no-slip condition at that boundary. This has important consequences for ciliary propulsion because of the different forms of image systems for stokeslets oriented normal and tangential to the wall as discussed in section (Blc). Since the far-field for normal stokeslets decays more rapidly

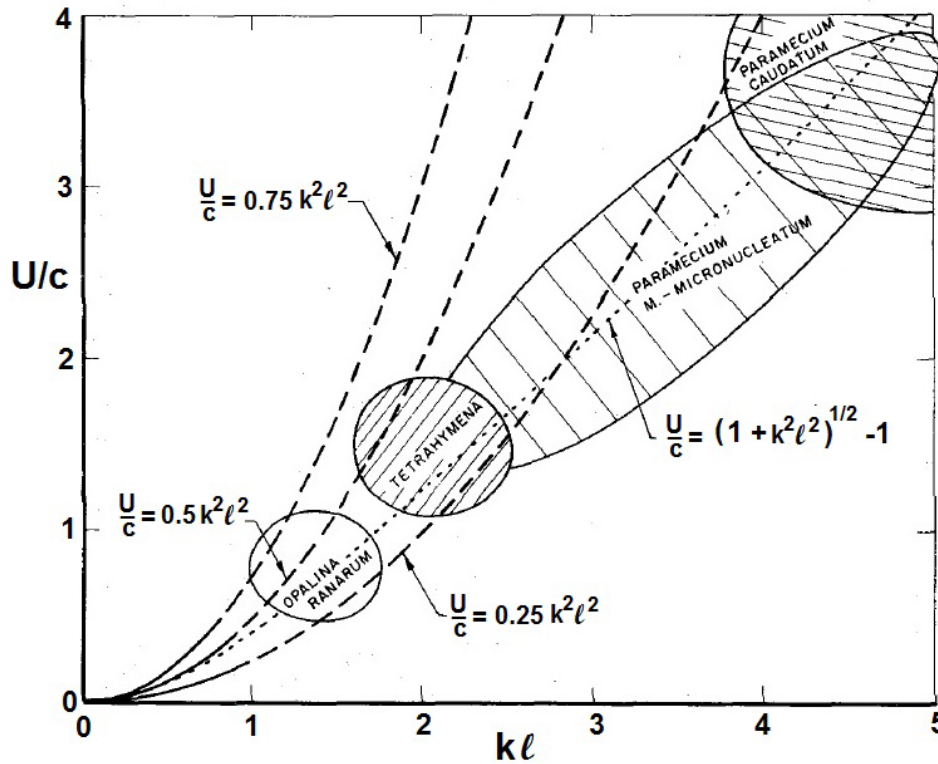


Figure 7: Comparison of the propulsive velocity of some ciliates (data given by areas denoting the scattering of the available information) with extrapolated predictions of envelope theories of the form $U/c \propto k^2 l^2$.

(like r^{-3}) than that of tangential stokeslets (like r^{-2}), it follows that the tangential motion of the ciliary elements is of much greater consequence than the normal motion.

The fluid-mechanical problem is constructed when the relative motion between an elemental length of cilium at a position \underline{x}_0 and its surrounding fluid is formulated in terms of a known cilium motion due to a specified beat pattern and the fluid velocity, $\underline{q}(\underline{x}_0)$. There is, however, a difficulty, here because the model presupposes that after a Galilean transformation utilizing $\underline{q}(\underline{x}_0)$ the element is translating as though in fluid at rest far from the element. This implies that the methods developed up to the present time must be limited to situations in which the cilia are sufficiently widely spaced so that the local flow field around one cilium does not extend to the neighboring cilia. One is left with the impression that such difficulties are not entirely resolved in the existing literature. Indeed, Blake & Sleight (1974) have pointed out that desirable improvements to the present sublayer models could be provided by studies of the translation of slender bodies in the presence of other similar bodies.

The above description suggests an iterative scheme that begins with a best guess for $\underline{q}(\underline{x})$ and proceeds through evaluation of the stokeslets to the calculation of a "new" velocity field, $\underline{q}(\underline{x})$. Such iterative methods have been used by Keller, Wu & Brennen (1975). Alternatively the problem may be put in the form of an integral equation for $\underline{q}(\underline{x})$ as originally demonstrated by Blake (1972).

In his sublayer analyses Blake (1972) included only a steady or time-averaged velocity of the fluid tangential to the wall, u , in his calculation of the stokeslet strength and obtained the steady velocity profile $u(x_3)$ (x_3 being the coordinate normal to the wall) that results from his solution of the integral equation. Keller, Wu & Brennen (1975) pointed out, however, that since oscillatory velocities of comparable and greater magnitude are created by the cilia motions these should be included in evaluation of the forces on individual cilium elements. They used a method somewhat different from that of Blake in which these forces are smoothed

out to form a continuous body force field within the cilia layer and their solution is achieved by solving the Stokes flow equations in this layer with these body force terms included. The resulting iterative solution yields a velocity profile not only for the steady velocities but, also for the oscillatory velocities both normal and tangential to the wall.

The solutions are all obtained in a frame fixed in the organism so that $u(\infty)$ is the propulsive velocity of the ciliary system. Indeed a particular feature of all the present infinite-sheet sublayer models is that $u(x_3)$ remains constant beyond the maximum extent of the ciliary tips. The majority of existing solutions are also for purely planar cilia beat patterns and for purely symplectic or antiplectic metachronism. As observed earlier, virtually all beat patterns contain to some greater or lesser degree displacements in all three coordinate directions and have metachronal patterns that deviate toward the diaplectic. Velocity profiles were derived by Blake (1972) and Keller, Wu & Brennen (1975) for *Opalina* and *Paramecium*. In both cases there are practical difficulties because the cilia of *Opalina* are too densely packed (see Figure 2) for one to have confidence in the sublayer model as presently constituted, and in the case of *Paramecium* because the metachronism is diaplectic and the beat three-dimensional (see above). The latter point was later rectified by Blake (1974a) who incorporated three-dimensionality in a sublayer model for *Paramecium*.

Ciliated Organisms

Apart from the infinite-sheet geometries discussed above several attempts have been made to apply these models to finite organisms. In the first solution of this kind Blake (1971a), extending earlier work by Lighthill (1952), approximated small- amplitude traveling waves on a spherical body by combining two spherical-harmonic functions whose orders differed by one. This envelope model is rather restrictive in terms of the permitted variation of wave form and amplitude and it approximates traveling waves only near the maximum width of the body. Subsequently Brennen (1974, 1975) pointed out that the flow around most ciliated organisms for which the metachronal wavelength is small compared with the overall dimensions will be comprised of two parts: (a) a relatively thin oscillatory boundary layer within which the oscillatory motions created by the cilia will decay rather rapidly with distance from the surface and (b) an outer steady Stokes flow around the organism. The problem is then to find some way of matching a local fluid/cilia interaction model within the boundary layer to the so-called complementary Stokes flow outside the boundary layer. For self-propelling organisms this complementary Stokes flow and the velocity of propulsion can only be obtained explicitly after application of the condition of zero total force on the organism; the velocity field far from the organism in this case probably cannot be like a stokeslet since the self-propelling organism exerts no net steady force on the fluid. On the other hand, if the organism is pinned down, the complementary Stokes flow will be like that of a stokeslet in the far field and the thrust produced by the restrained organism can be computed. Brennen (1974, 1975) has applied such a matching technique to the propulsion of spherical and ellipsoidal ciliates using an envelope model for the local fluid/cilia interaction and Blake (1973a) has considered the effect of a finite cell body on results obtained for infinite-sheet models.

One particular feature of Brennen's results (1974, 1975) is that they allow evaluation of the thrust, T , that a restrained organism can produce. [With regard to this it is worth noting, as Taylor (1951) did, that there is zero net thrust in the infinite-sheet solutions.] Typical values from an envelope model are shown in Figure 8 for direct comparison with Figure 6. Note that the ciliary beat patterns for optimum thrust on restrained organisms differ from those for optimum rectilinear propulsive velocity. This raises questions of whether a large starting (or turning) thrust or an optimum steady propulsive velocity is of greater importance for individual species.

Perhaps the simplest demonstration of an envelope or traction layer model applied to a finite organism is to consider a ciliated spherical organism moving through a fluid at very low Reynolds and whose surface

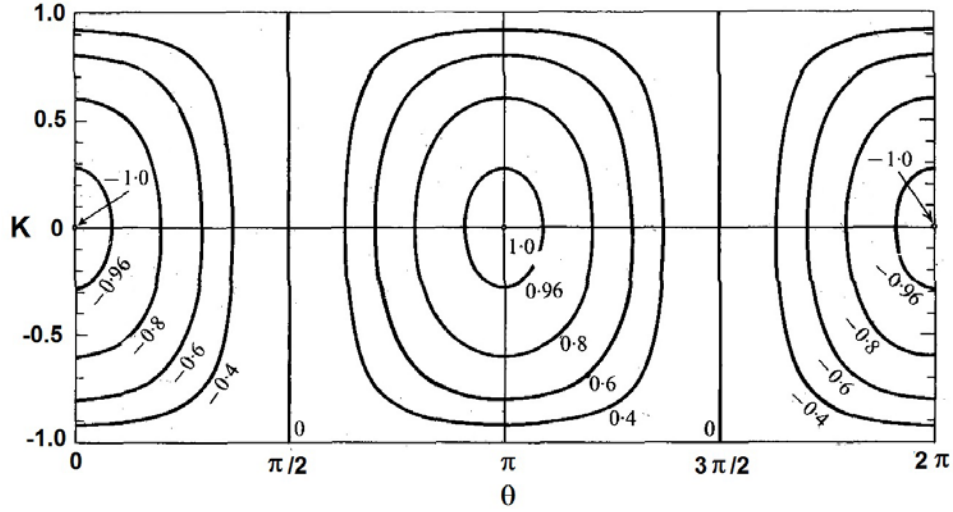


Figure 8: Typical contours of the nondimensional thrust, $3T/4\pi\mu k^2(h_s^2 + h_n^2)Ac$, where T is thrust developed by a restrained ciliate of typical dimension $2A$, according to an envelope model for the fluid/cilia interaction (Brennen 1975). For comparison with Figures 5 and 6.

cilia create an effective tangential surface velocity of $U^* \sin \theta$ where θ is the angle measured from the front stagnation point. [This could also be used as a model for an organism like and amoeba that generates new surface and creates a similar tangential surface velocity.] Since the organism is moving at very low Reynolds number, we can deploy a Stokes' stream function.

$$\psi = \sin^2 \theta \left[-\frac{Ur^2}{2} + \frac{A}{r} + Br \right] \quad (\text{Dfh4})$$

and the corresponding velocity components in the radial and tangential directions:

$$u_r = \frac{1}{r^2 \sin \theta} \frac{\partial \psi}{\partial \theta} = \cos \theta \left[-U + \frac{2A}{r^3} + \frac{2B}{r} \right] \quad \text{and} \quad u_\theta = -\frac{1}{r \sin \theta} \frac{\partial \psi}{\partial r} = \sin \theta \left[U + \frac{A}{r^3} - \frac{B}{r} \right] \quad (\text{Dfh5})$$

Since the organism is moving at a constant velocity, the sum of forces in that direction must be equal to zero. To evaluate this the total force, we need to integrate the shear and normal stresses over the surface of the organism. In axisymmetric, spherical coordinates the shear stress, $\tau_{r\theta}$, is given by:

$$\tau_{r\theta} = \mu \left(\frac{1}{r} \frac{\partial u_r}{\partial \theta} + \frac{\partial u_\theta}{\partial r} - \frac{u_\theta}{r} \right) \quad (\text{Dfh6})$$

and substituting the above velocity components:

$$\tau_{r\theta} = -6\mu \sin \theta \frac{A}{r^4} \quad (\text{Dfh7})$$

To find the normal stress, we integrate the zero Reynolds number equations of motion to obtain the pressure distribution in the fluid:

$$p(r, \theta) = \int \left(-4\mu \cos \theta \frac{B}{r^3} \right) \partial r = 2\frac{\mu B}{r^2} \cos \theta + \text{constant} \quad (\text{Dfh8})$$

Far from the organism ($r \rightarrow \infty$), the pressure is equal to the ambient pressure, p_∞ , so the pressure distribution around the organism is given by:

$$p(r, \theta) = p_\infty + 2\frac{\mu B}{r^2} \cos \theta \quad (\text{Dfh9})$$

Then the net force in the horizontal direction is given by:

$$F_x = - \int_0^\pi \tau_{r\theta}|_{r=R} \sin \theta \, 2\pi R^2 \sin \theta d\theta - \int_0^\pi p|_{r=R} \cos \theta \, 2\pi R^2 \sin \theta d\theta \quad (\text{Dfh10})$$

which yields

$$F_x = \frac{4}{3}\pi R^2 \mu \left(12 \frac{A}{R^4} - 4 \frac{B}{R^2} \right) \quad (\text{Dfh11})$$

Setting this equal to zero since there is no net force on the organism yields the first relation between the constants A and B :

$$A = \frac{1}{3}BR^2 \quad (\text{Dfh12})$$

In addition the no-slip condition ($u_\theta(r = R) = U^* \sin \theta$) at the surface gives:

$$\sin \theta \left(U + \frac{A}{R^3} - \frac{B}{R} \right) = U^* \sin \theta \quad \text{or} \quad B = \frac{3}{2}R(U - U^*) \quad (\text{Dfh13})$$

The condition on the normal velocity at the surface gives:

$$\cos \theta \left(-U + 2\frac{A}{R^3} + 2\frac{B}{R} \right) = 0 \quad \text{or} \quad U = 2\frac{A}{R^3} + 2\frac{B}{R} \quad (\text{Dfh14})$$

Combining the results (Dfh12), (Dfh13) and (Dfh14) allows evaluation of the velocity, U , at which the organism moves through the liquid:

$$U = \frac{2}{3}U^* \quad (\text{Dfh15})$$

Thus the organism will move forward through the fluid with a velocity that is $2/3$ of the maximum slip velocity generated at the surface.